JOURNAL OF MATERIALS SCIENCE 10 (1975) 63–76

An investigation of the relationships between processing conditions, microstructure and mechanical properties of an injection moulded semi-crystalline thermoplastic

J. BOWMAN, N. HARRIS, M. BEVIS
Department of Metallurgy and Materials Science, The University of Liverpool, UK

The semi-crystalline polymer TPX has been injection moulded into standard tensile bars using a range of barrel temperatures, mould temperatures and injection pressures. Acid etching, microhardness testing and selected volume X-ray pole figures were used to characterize the changes in microstructure and crystalline texture which occurred throughout the range of mouldings. A strong correlation was shown to exist between microstructure and crystalline texture and processing conditions. Three-point bend tests on the injection moulded bars indicated that a ductile-to-brittle transition in failure mode could be induced by changing the moulding conditions, and that this change could be correlated with microstructural and dimensional changes.

1. Introduction

The variations in flow rates and cooling rates occurring in the fabrication of a plastic component give rise to variations in the microstructure and, therefore, the mechanical and physical properties of that component. The objective of the research leading to the results presented, was to identify the relationships between the injection moulding variables, microstructural variations throughout a component, and the mechanical properties of a component injection moulded from a semi-crystalline thermoplastic. The semi-crystalline thermoplastic was TPX, a commercial co-polymer based on poly-4-methyl pentene-1, and purchased from ICI. Poly-4-methyl pentene-1 has a tetragonal crystal structure [1] with unit cell dimensions of $a = b = 18.6$ Å and $c = 13.8$ Å when the molecular chain axes are parallel to the c-axis. Moulded components of TPX are transparent, and optical microscopy could, therefore, be used to locate and characterize some of the deformation modes operating within the component. This offers a considerable advantage over previous investigations of semi-crystalline thermoplastics [2-6], where relationships between moulding variables and microstructure have been found; but the correlation between fine microstructural changes through the thickness and the operative deformation mechanisms could not be considered.

Although two types of moulding have been investigated, an A.S.T.M. tensile test bar (A.S.T.M. D638–68) and a 4 mm thick plaque, this paper is restricted to a description of the identification procedures for, and the annotation of, the microstructural changes occurring in the A.S.T.M. tensile bars when the moulding variables (barrel temperature, injection pressure and mould temperature) are varied in a systematic way. A description of the results of three-point bend tests on the A.S.T.M. tensile bars demonstrates in a clear way that a ductile-to-brittle transition in failure mode can be induced by changing the moulding conditions, and that this change can be correlated with microstructural changes.

This paper represents an extension of previous studies by Owen and Hull [7], co-workers of the present authors, who considered in detail the failure mechanisms of plaques moulded from TPX under one set of moulding conditions.

2. Specimen preparation

2.1. Moulding

Tensile bars, to A.S.T.M. standard D638–68 type 1, were moulded in TPX (grade RT18) using a BIP (Bipel 60/26) injection moulder, with barrel temperatures set at values of 533, 553, 573, 593 and 613 K using two injection pressures, 68 and 122 MN m^{-2}, with a mould temperature of 293 K. For the barrel temperatures 533, 573 and 613 K with the 68 MN m^{-2} injection pressure, the mould temperature was raised to 313, 333 and 353 K to produce additional mouldings. The manufacturer's generally recommended injection moulding processing conditions were 543 to 598 K for the barrel temperature, and 333 to 353 K for mould temperature. (For convenience the conditions of specimen moulding will subsequently be given in the shorthand form of barrel temperature, injection pressure, mould temperature.) The moulding conditions quoted were as read from the control panels; for the direct monitoring of temperature or pressure of the melt in the mould, no facilities were available.

2.2. Etching studies

Etch figures, together with microhardness profiles and selected volume X-ray pole figures were used as the primary means of characterizing the microstructure and crystalline texture in the range of mouldings referred to above. For etching studies, the A.S.T.M. tensile bars were cut, as shown in Fig. 1, with a jeweller's saw, to reveal a surface parallel to the injection direction and lying in the narrow section of the bar. The surface was ground to 600 emery paper, then polished on diamond paste wheels to $\frac{1}{4}$ μm. The polished surface was examined in an optical microscope to ensure it was free from gross (1 to 2 μm) scratches.

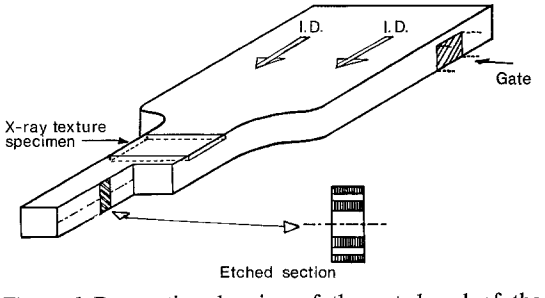

Figure 1 Perspective drawing of the gated end of the A.S.T.M. bar showing the position of the plane in the narrow section from which the etch patterns were obtained, and the orientation of the X-ray texture specimens relative to the bar and the etched sections. I.D. denotes the injection direction.

2.3. Microhardness plots

The surface defined in Section 2.2 was exposed, and the specimen mounted in a polishing jig with 1 mm thick sheets of compression moulded TPX either side. This composite specimen was then ground to 600 emery and 1 μm diamond paste, yielding a job having the injection moulded specimen intimately sandwiched between material of very nearly the same hardness, so reducing the obvious possible edge effect.

2.4. Texture determination

For X-ray texture determination specimens, the position of the structure to be examined was determined from (a) the low magnification optical micrographs of the etched sections, and (b) the microhardness profiles. The determined amount of material was hand polished away from each side of the specimen, using wet emery, isolating the desired structure. Specimen thickness was in the range 80 to 150 μm, the breadth 12.5 mm and the length, a minimum of 10 mm, with a specimen orientation relative to the injection direction as shown in Fig. 1.

The selection of particular specimens by use of the selective etching results and microhardness plots greatly facilitates the characterization of the crystalline textures through the thickness of the mouldings. The effectiveness of sledge microtomy and the use of an abrasive saw as techniques for the preparation of X-ray texture specimens were also examined. The problem of knowing the exact position of the specimen relative to the surface of the mouldings negated the use of these techniques. However, for specimens moulded under similar conditions and from identical positions within the bar (i.e. the surface skin), all three sample preparation techniques gave identical textures, vindicating the first specimen preparation technique described.

2.5. Bend tests

The specimens for bend testing were in the as-moulded condition except both sides of the specimens were polished with wet emery down to 600 grade then $\frac{1}{4}$ μm diamond paste. This enabled the operating deformation modes through the thickness of the specimen to be observed. The minimum amount of material was

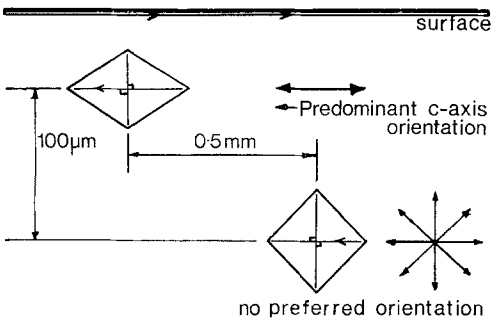

Figure 2 Schematic diagram showing the orientation of the microhardness indentations relative to the top surface of the bar. The injection direction is horizontal with the separation of successive indentations shown. The oriented and equiaxed structures present in moulding cause the indentations to change shape as shown.

removed from each side, consistent with the requirement for viewing. The specimens were approximately 3.1 mm thick and 12.5 mm wide.

3. Specimen testing and examination

3.1. Acid etching

The specimens prepared according to Section 2.2 were etched in a 6 M CrO_3 solution for at least 9 h. The temperature of the solution was the reflux temperature, 377.5 K.

3.2. Vickers microhardness testing

The acid etching technique is relatively long in its application and alternative but more rapid ways of characterizing changes in the microstructure of mouldings were considered. Vickers microhardness testing proved to be the most satisfactory and the procedure adopted was that used extensively by metallurgists for characterizing the hardness changes in metals [8].

The technique essentially consists of monitoring the dimensions of the impression which results when a pyramid-shaped indentor is placed, under a constant load, on a selected area of the specimen. The dimensions measured are the diagonals of the observed diamond-shaped indentation (see Fig. 2) and the hardness H is proportional to W/d^2, where d is the size of the diagonal (μm) and W is weight (g), required for making the indentation. For an anisotropic material, the diagonals will be of unequal length, as in Fig. 2, so that the hardness values have to be calculated for the individual diagonal, rather than averaging pairs. The spherically symmetrical strain field produced by the Vickers microhardness indentor responds to anisotropy in the material [9], and this was the sagacious rationale behind its use for assessing microstructural and molecular structure variations throughout a moulding. The microhardness indentation is sufficiently small to allow it to exist within and respond to changing morphologies and anisotropies. Fig. 2 illustrates this response to anisotropy in a moulding, the structure of which is explained later, and the figure also shows how the indentor was aligned so that one diagonal was parallel and one perpendicular to the injection direction. At least four sets of indentations, 100 μm centre-to-centre apart, were made across each specimen and the results were in all cases consistent from one set to another.

3.3. Texture

X-ray analysis based on the determination of pole figures using an X-ray diffractometer is becoming a widely used tool for the texture investigation of crystalline polymers [10-12]. The preferred orientations of chosen sets of lattice planes are clearly mapped out in a well-defined manner when a pole figure is produced. Data analysis by computer and automatic graph plotting can lead to the rapid production of processed results. In the determination of the pole figures presented in Section 4.4, a Siemens Texture goniometer with a 344 mm diameter measuring circle was used both in the back reflection and transmission modes. Pole figures were prepared from the thin samples of the type described above to determine the preferred orientation of the (200) and (212) poles. Vanadium-filtered $K\alpha$ radiation was employed and intensities were recorded from a gas-filled proportional counter. The planes selected for pole figure determinations have lattice spacings of 9.3 and 5.3 Å and formed diffraction peaks at Bragg angles of 7° 2′ and 12° 30′ respectively.

In transmission the procedure adopted was to explore first the presence of (200) planes whose normals were in the specimen surface ($\alpha = 0$) [13] by scanning the vertical circle of the goniometer at 30° per minute through 360°, then to explore the presence of (200) planes whose normals made an angle of 5° with the specimen normal ($\alpha = 5°$) and so on at 5° intervals up to $\alpha = 40°$. In back reflection, the well-known helical plot was produced commencing at $\alpha = 20°$ and continuing towards $\alpha = 90°$ with 5° steps between each turn of the helix.

The product of the thickness t and the

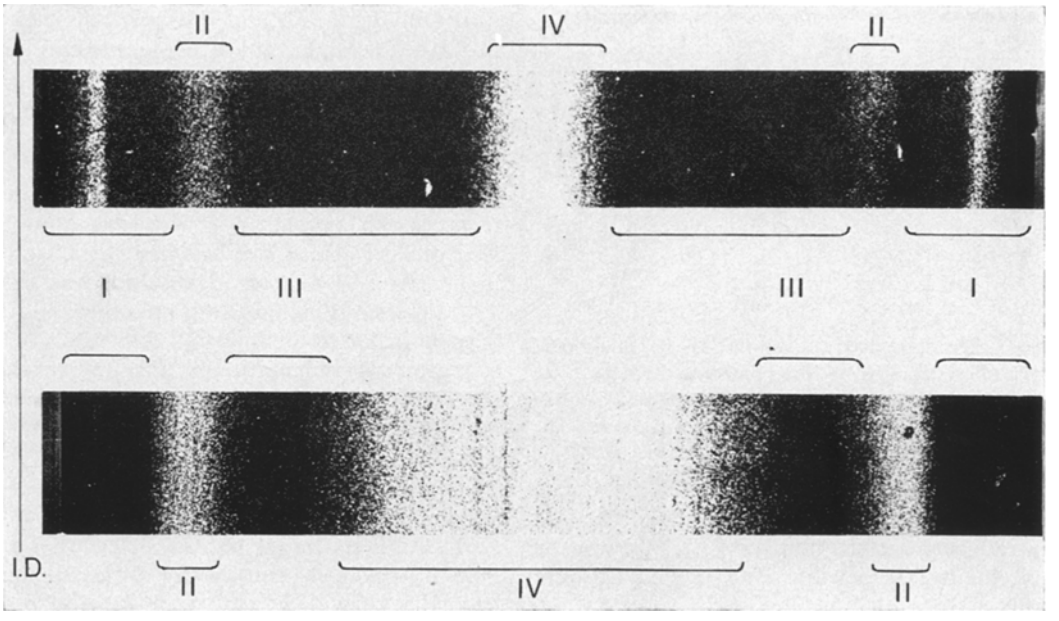

Figure 3 Low magnification (× 70), reflected-light photographs of bars moulded at 553-68-293 (top) and 593-68-293 (bottom). The areas of low reflectivity (regions I and III) possessed a preferred orientation while the areas of high reflectivity (II and IV) are equiaxed. I.D. as shown.

absorption coefficient μ for each specimen was determined by the usual method of determining the ratio of the intensity of a beam when passed through the specimen with that of the same beam when the specimen is absent. These figures were typically $\mu t = 0.1$ and were used in the standard correction procedures for back reflection and transmission methods [14]. Background levels were determined in each case and subtracted from the intensities recorded at the Bragg angle.

In order to obtain correspondence between the pole figures, the contours were plotted in such a way that each contour represents a certain intensity above the background radiation level. Thus, when the preferred orientation is high, as many as twelve contours appear; when it is low only a few are recorded.

3.4. Bend tests

The A.S.T.M. bend test specimens, prepared as in Section 2.5 were tested in a three-point bend testing jig [15] at a cross-head speed of 10 mm min^{-1} with an L/D ratio of 16 and a span of 50 mm. The test was carried out for at least 90 sec producing a calculated strain in the outer fibre of 10.8%.

Bend testing as a means of characterizing the mechanical properties of the moulded bars was used because the rapid testing possible allowed good temperature control during the testing of specimens moulded under all of the moulding conditions. A visual examination of some of the deformation modes, and their position within the specimen, was made during the test.

4. Experimental results and discussion

4.1. Low magnification reflected optical photographs

Etch studies of that section of the TPX moulded A.S.T.M. bar illustrated in Fig. 1 showed that for all moulding conditions, the sections were composed of two main classes of microstructure: a highly oriented structure and a crudely developed spherulitic structure. These two structures were present in the low-magnification reflected-light optical photographs of etched section of the material moulded at 553-68-293 and 593-68-293 (i.e. barrel temperature K, injection pressure MN m^{-2}, mould temperature K) and they are shown in Fig. 3. The areas of low reflectivity are the highly oriented regions (I and III) while the areas of high reflectivity, with the exception of the narrow band at about 180 μm from the surface, are the regions which exhibit the crudely developed spherulitic or equiaxed structure (regions II and IV). Although the intensity of the band near the edge of the

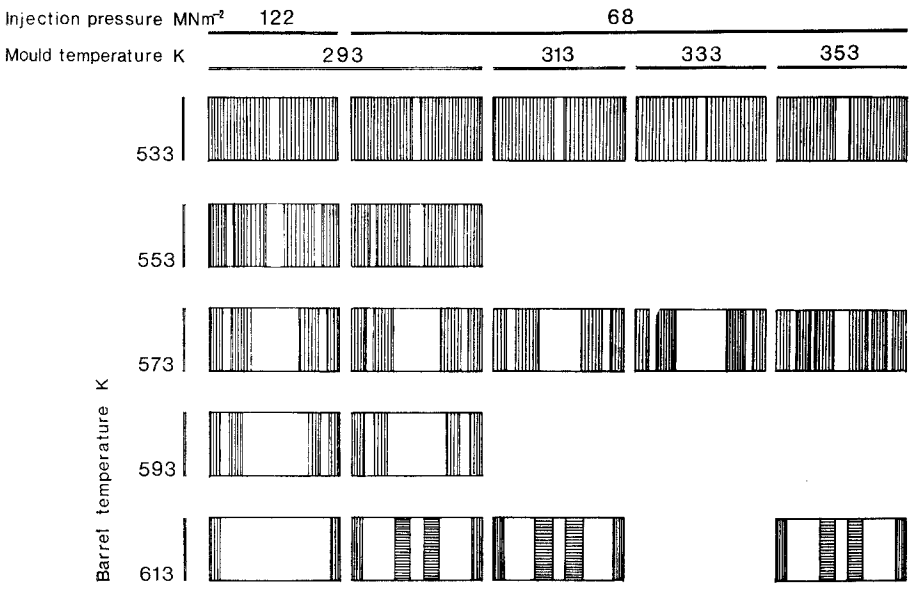

Figure 4 Schematic representation of the positions and extents of the oriented and equiaxed structures, drawn from three low-magnification reflected-light photographs for all moulding conditions. The hatched areas are oriented, the direction of hatching denoting the predominant direction of the *c*-axis. The influence of moulding conditions upon the structures and their distribution is self-evident. I.D. is vertical.

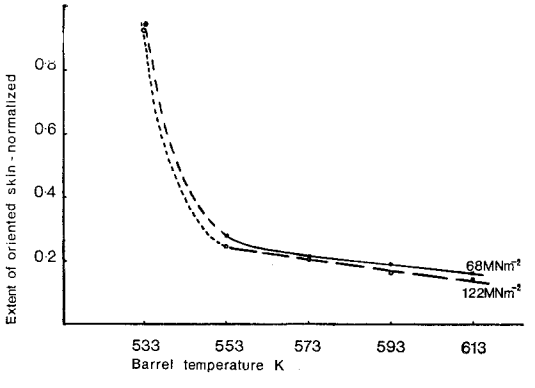

Figure 5 The fraction of the etched section of the bar occupied by the highly oriented skin, as a function of barrel temperature. The top plot is for an injection pressure of 68 MN m^{-2}, the bottom plot, 122 MN m^{-2} with a mould temperature of 293 K in both cases.

specimen decreased with increasing barrel temperature it always exhibited an oriented structure.

The photographs shown in Fig. 3 can be represented in the schematic form of Fig. 4, which summarizes the differences in the distribution of oriented and spherulitic structures, with differences in moulding conditions. As with Fig. 3, the regions of dark contrast correspond to the highly oriented regions, and the light contrast areas are the equiaxed regions. The main conclusions that can be drawn from these results are:

(a) Centre structure (region IV). The extent of the equiaxed centre region of the moulding increases with barrel temperature, for both moulding pressures, in the range 533 to 593 K.

(b) Edge equiaxed structure (region II). With the barrel temperature set at 553 K, this additional region of equiaxed structure is inducted at about 420 μm from the surface, the extent of the region increasing linearly up to 593 K barrel temperature. At 613 K, the centre and edge equiaxed structures meet. For both injection pressures, the distance of the equiaxed edge structure from the surface of the bar decreases linearly with increasing barrel temperature as illustrated in Fig. 5.

(c) Total extent of equiaxed structure. This is found to increase linearly with barrel temperature in the range 533 to 593 K for both injection pressures, as shown in Fig. 6.

(d) Injection pressure. An increase from 68 to 122 MN m^{-2} for the packing pressure (the cycle always commences with a peak pressure of 122 MN m^{-2}) causes a small decrease in the volume of oriented material (regions I and III) as illustrated in Fig. 6.

(e) Mould temperature. For the 533 K barrel

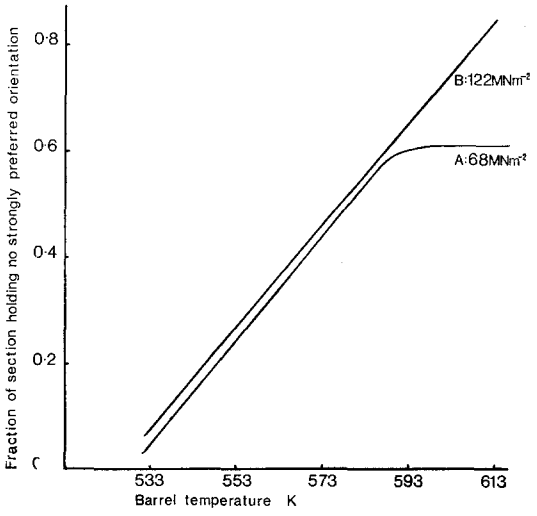

Figure 6 The fraction of the etched section of the bar occupied by the equiaxed structure, as a function of barrel temperature, for the two injection pressures (A = 68 MN m^{-2} and B = 122 MN m^{-2}) at mould temperature of 293 K.

temperatures, the effect of raising the mould temperature from 293 to 353 K is to cause no discernible change or drift in the extent of the equiaxed centre structure. At a barrel temperature of 573 K, the effect of raising the mould temperature has little effect until the mould temperature reaches 353 K. Then, the amount of oriented material sharply increases. At a barrel temperature of 613 K the mould temperature exerts no discernible effect.

All of the observations reported above and presented in Fig. 4 were recorded from etched material from that part of the narrow section of the A.S.T.M. moulded bar nearest the gate: the average of at least three micrographs from three different bars and from this zone were used. In addition, one of the three etched bars was used to provide a section from that part of the narrow section furthest from the gate. The difference between the morphology distribution of the cross-sections obtained near the gate and far from the gate, for a 68 MN m^{-2} injection pressure, was of approximately the same magnitude and same direction as the difference between the two injection pressures, as illustrated in Figs. 5 and 6.

As stated earlier, no monitoring and, therefore, no fine control facilities existed to confirm and control the slender changes in melt temperature and injection pressure that occur naturally when moulding under one condition. By subaudition, a variation in the micromorphology from sample to sample for any one moulding condition was anticipated and Fig. 7 shows the variations in etched structures that occur for moulding at

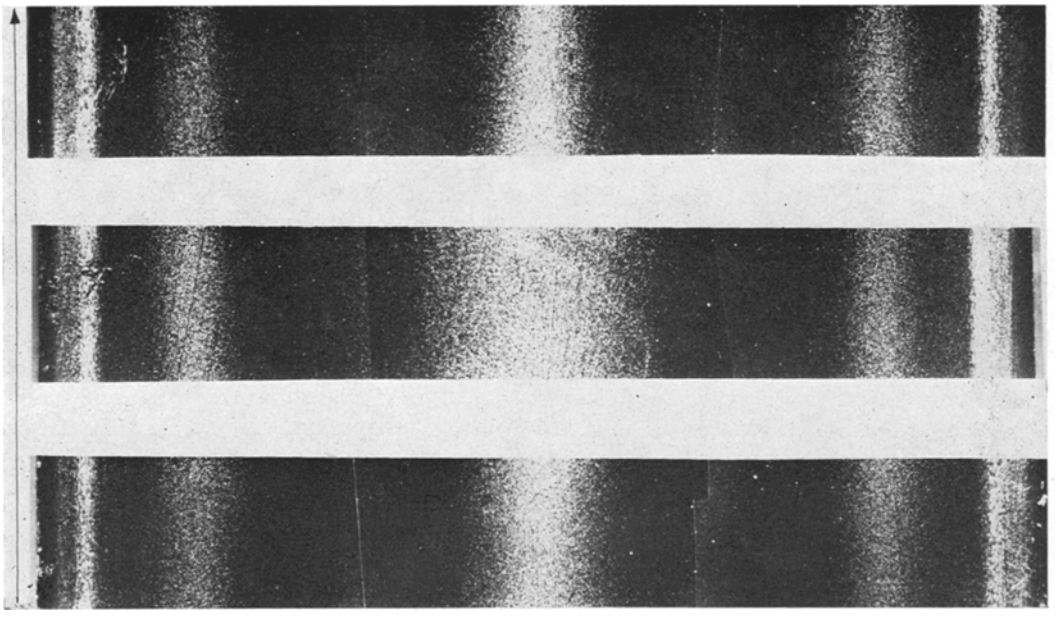

Figure 7 Three low-magnification (× 70), reflected-light photographs from the etched sections of three bars moulded at 553-122-293 showing the bar-to-bar variations in structure distributions. I.D. is vertical.

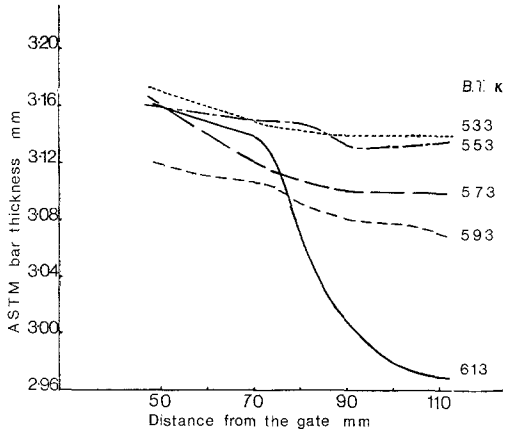

Figure 8 The thickness of the bar as a function of distance from the gate at various barrel temperatures. The injection pressure was 68 MN m^{-2} and the mould temperature 293 K for all mouldings. The mean of five readings was used for each thickness plotted.

553-122-293. The changes in micromorphology distribution are not extensive and when error bands are inserted into Fig. 6, no overlap occurs for either plot.

Mention must be made of the moulding at 613-68-293 which, by extrapolation from Fig. 6, should consist simply of a crudely developed spherulitic core and an oriented skin. This was substantially the case, except that towards the centre, a narrow oriented band existed (region V in Fig. 13a), having a width of about 300 to 400 μm and being about 1 mm from the surface on both sides (see Fig. 13a). This band was shown to have the molecular chain axis, the *c*-axis of the unit cell, oriented perpendicular to the injection direction and, in addition, it was found to be most extensive near the gated end, practically disappearing at the closed end of the A.S.T.M. tensile specimen. Measurement of the change in thickness of the bar with point of measurement from the gate showed that the absence of this structure for a high melt temperature led to large specimen dimensional changes, as is illustrated in Fig. 8. In addition Fig. 8 shows that there is a correlation between melt temperature and component thickness stability, when measuring the thickness of the narrow section: each thickness value represents the average of five readings.

4.2. Microhardness profiles

Using the section of the A.S.T.M. bar used for the etching studies, microhardness profiles were obtained for material moulded under the

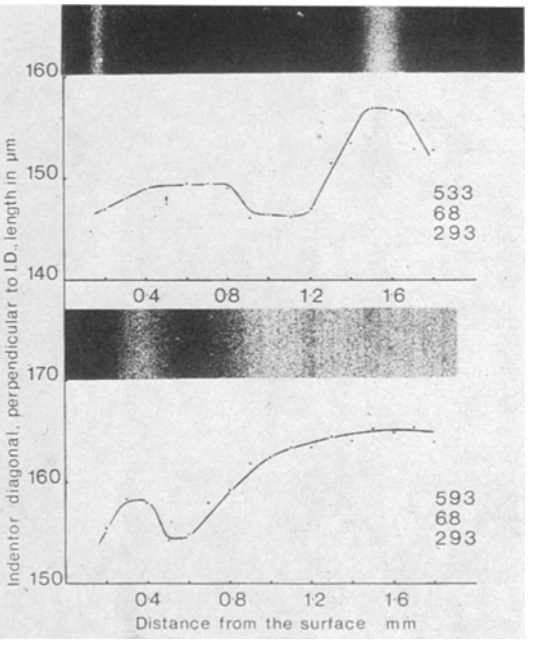

Figure 9 Photographs of the etched bars, coupled with the microhardness profiles (an average of four plots) from the equivalent position within the bar illustrate the correlation between the two techniques for bars moulded at 533-68-293 (upper) and 593-68-293 (lower).

following five conditions (533, 553, 573, 593, 613)-68-293. Measurement of that diagonal perpendicular to the injection direction, adopting the technique described in Section 3.2, yielded microhardness profiles that matched the corresponding photographs of the etched specimens. Fig. 9 pairs the microhardness plots and photographs from equivalent positions in the bar, for two moulding conditions, (533-68-293) and (593-68-293). The abscissa in Fig. 10 plots the mean value (drawn from at least four plots) of the diamond diagonal size (d) for the diagonal perpendicular to the injection direction with respect to the structure variations for two average temperatures of testing, 299.5 and 292 K. However, it can be seen that in the plots for both temperatures the maximum and minima correspond to the same positions within the bar, reflecting the structural variations.

Further proof of the efficiency of microhardness plots for characterizing the microstructural variations in injection moulded specimens is provided when characterizing the material moulded at 613-68-293. This moulding has a skin oriented with the *c*-axis parallel to the injection direction, and a crudely developed

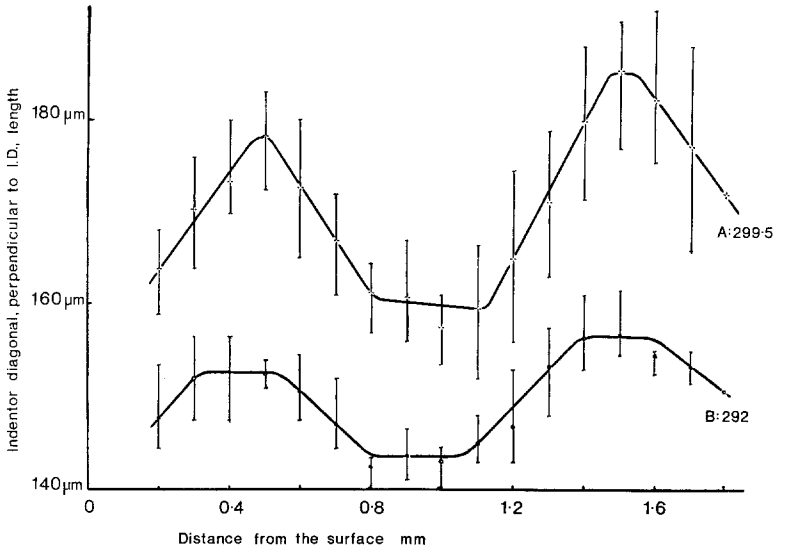

Figure 10 For moulding at 553-68-293 the variations in diamond diagonal lengths as a function of position within the bar, together with arrow bars for each point, for two temperatures of conducting the indentations; A is 299.5 K and B is 292 K.

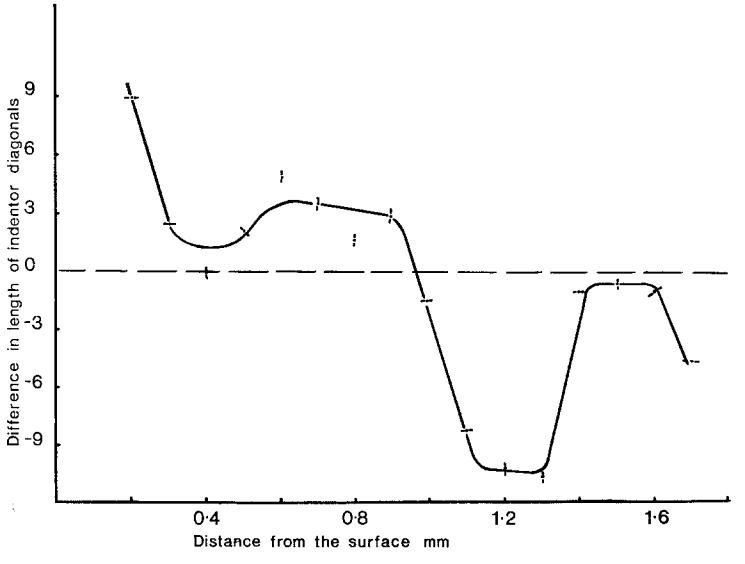

Figure 11 The difference in the length of the indentor diagonals perpendicular and parallel to the injection direction as a function of position within the bar for the 613-68-293 moulding.

spherulitic core which contains a narrow oriented band having the *c*-axis perpendicular to the injection direction (see Fig. 13). A microhardness plot, measuring the difference in the length of the diagonals parallel to and perpendicular to the injection direction for this moulding, clearly reflects the changes in orientation, as can be seen in Fig. 11.

4.3. High resolution microscopy

Scanning electron microscopy studies showed that all etched sections of all of the tensile bars examined exhibited only two classes of microstructure, an oriented and non-oriented structure, both highly crystalline. Figs. 12a and 13a show the low-magnification reflected-light optical photographs of the etched sections of bars

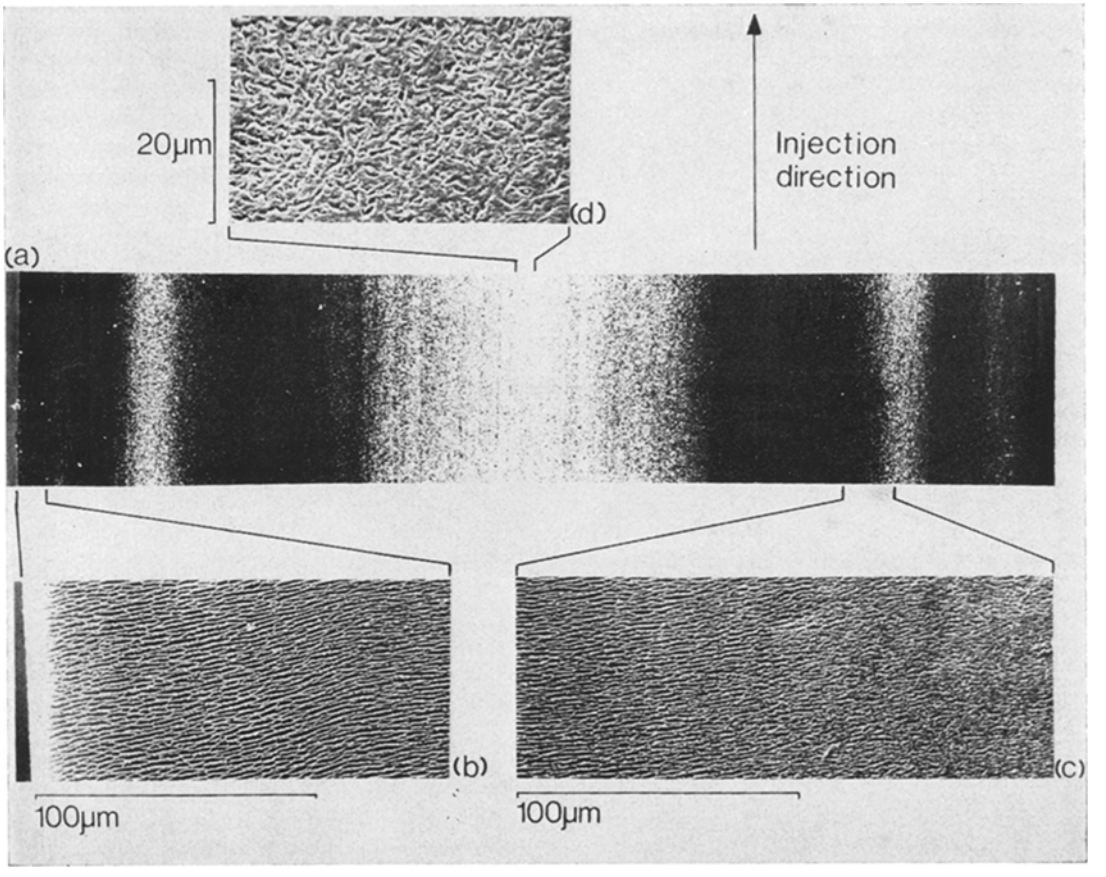

Figure 12 For the 573-68-293 moulding (a) the low magnification (× 65) photograph in reflected light of the etched plane, (b) an SEM of region I, (c) an SEM of regions II and III, and (d) an SEM of region IV. The injection direction is vertical for all structures and the micrographs (b), (c) and (d) were taken from the etched plane shown in (a).

moulded at (573-68-293) and (613-68-293) respectively. Scanning electron micrographs which illustrate the microstructures exhibited by the component regions I to IV of the bar moulded at (573-68-293) are shown in Fig. 12b to d: component regions I, IV and V for the bar moulded at (613-68-293) are shown in Fig. 13b to d. These figures represent all the structures that have been isolated as being present in TPX injection mouldings prepared on the machine named and into the shape indicated and under the conditions annotated. Regions I, II (where applicable) and III exhibited a "row structure" morphology which occurs in semi-crystalline polymers as a result of crystallization under a melt shear or elongational strain [16-19]. Region V which only occurs for moulding at 613-68 results from tensile shrinkage stresses which are more pronounced at higher barrel temperatures. The predominant orientation of the rows was always found to be normal to the molecular chain axis as determined by the X-ray pole figure studies.

The scanning electron micrograph in Fig. 14 was recorded for a different relative orientation of specimen and optical axis of the SEM to those shown in Figs. 12 and 13. The micrograph was obtained from region I of the material moulded at 593-68-293 and it has been possible to observe individual lamellae within the non-planar sheaf-like structure. This type of morphology was present as the outer skin for bars moulded at the barrel temperatures 533 to 593 K. The parallelism of the rows did vary with moulding conditions and position in the specimen, but the reproducibility of the etching procedure was not sufficiently good to quantify these differences. There was a strong tendency, however, for the

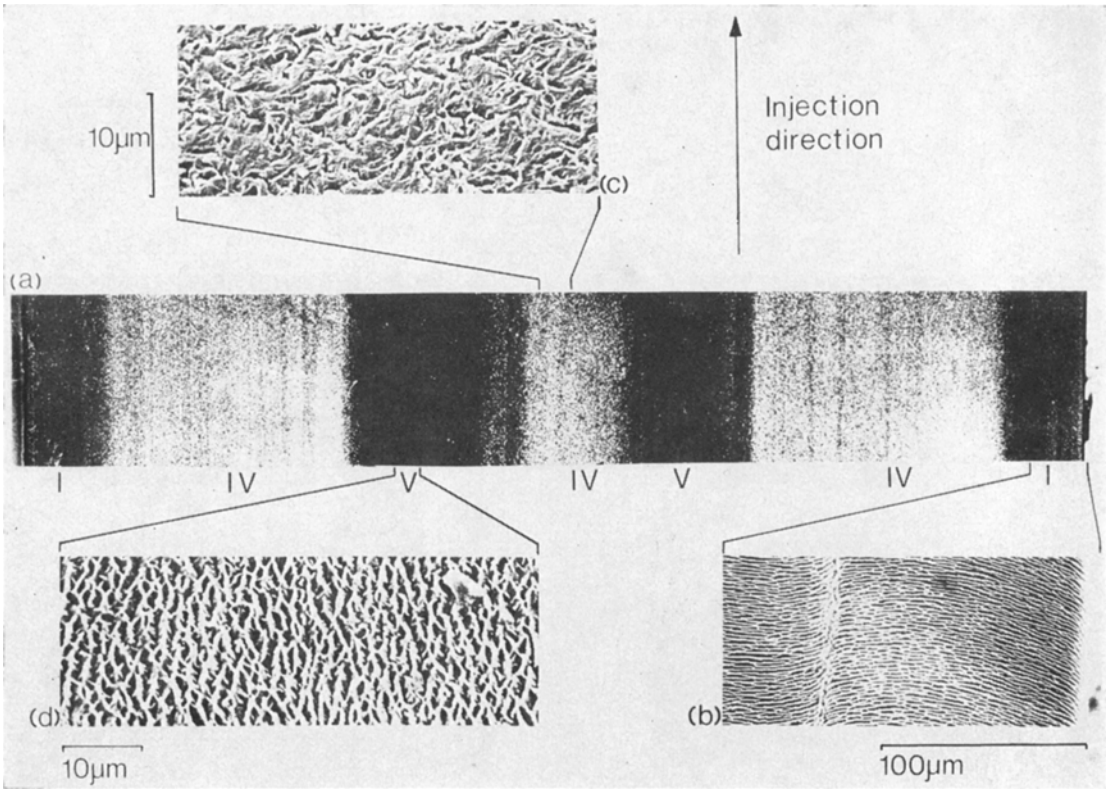

Figure 13 For the 613-68-293 moulding (a) the low magnification (× 65) photograph of the etched plane of Fig. 1 in reflected light, showing the regions of this moulding, I, IV and V, (b) an SEM of region I, (c) an SEM of region IV, and (d) an SEM of region V. The injection direction is vertical for all micrographs and micrographs (b), (c) and (d) are taken from the etched material.

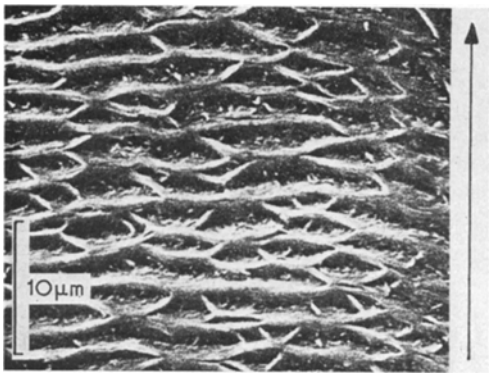

Figure 14 Scanning electron micrograph of region I of the material moulded at 593-68-293. The angle between the electron optical axis and specimen surface normal was reduced from about 55° (the angle used in Figs. 12b to d and 13b to d) to about 12° for this figure. I.D. is vertical.

parallelism of rows to decrease with respect to region in the order I, III, II with the rows in II exhibiting the least, if any, parallelism. Etch studies do provide sufficient information to meaningfully differentiate the bars into regions I to V, using the different forms of microscopy listed.

4.4. X-ray pole figures

The complete sets of (200) pole figures for regions I to IV in the bars moulded under the conditions (553-68-293) are shown in Fig. 15. It is clear from the pole figures that the texture weakens with the position of the specimen in the bar, in the order I, III, II, IV with the poorly developed spherulitic region IV exhibiting the weakest texture as would be expected. The diffuse (200) pole figures obtained from regions I, III and II showed that for moulding at (553-68-293) the *a*- and *b*-axis of the crystalline regions made angles with the bar surface normal which were predominantly less than 45°. The diffuse (200) pole figures also showed a correlation between the strength of the crystalline texture and the parallelism of the row structure,

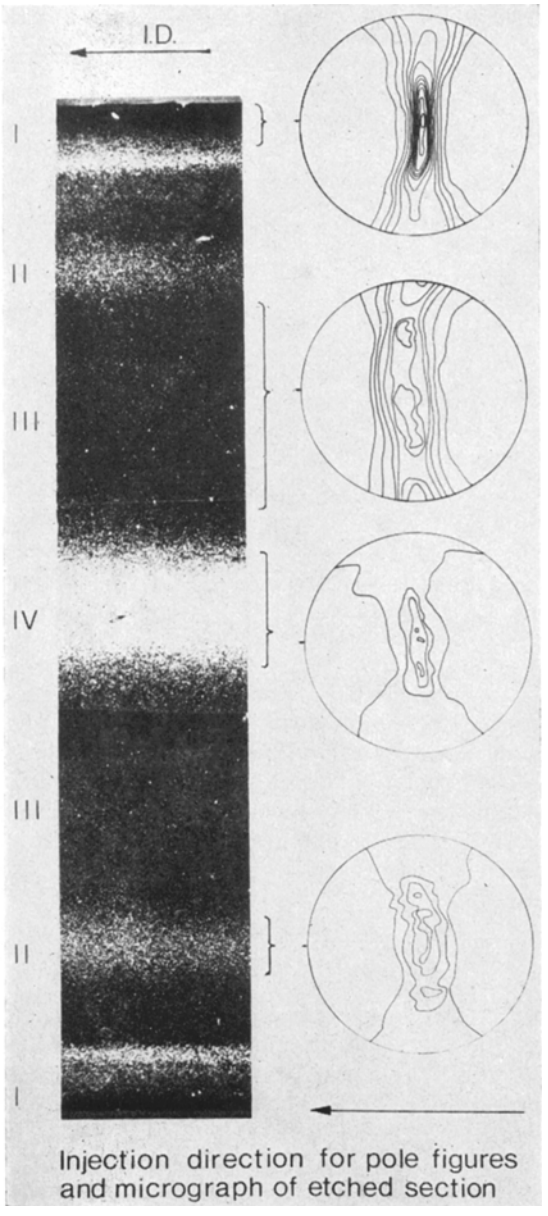

Figure 15 For the 553-68-293 moulding the low magnification (× 65) photograph of the etched plane together with the (200) pole figures for regions I to IV of that moulding.

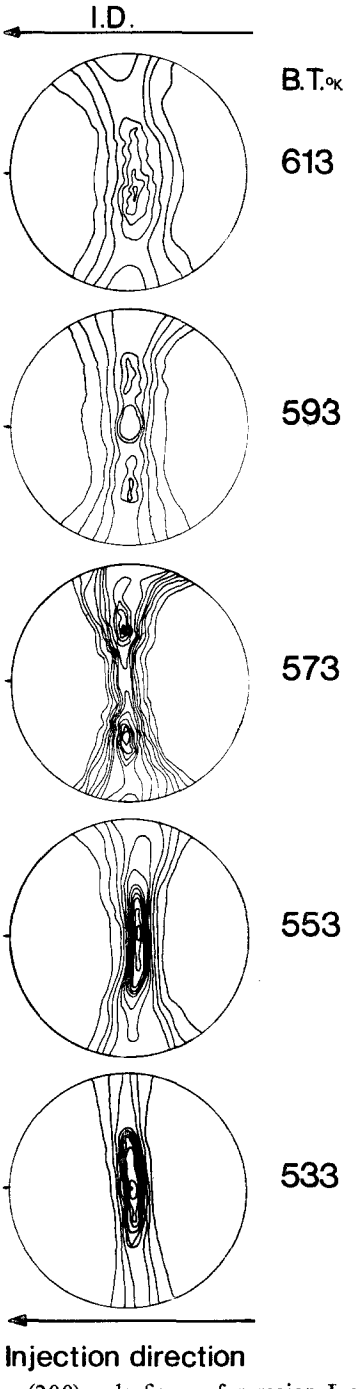

Figure 16 The (200) pole figures for region I of bars moulded at (613, 593, 573, 553 and 533)-68-293.

observed in the scanning electron microscope.

The (200) pole figures, obtained from the outer skins, for moulding at (533, 553, 573, 593 and 613)-68-293 are shown in Fig. 16 and show that the strongest textures are observed at the lowest barrel temperatures, the textures becoming progressively weaker with increasing barrel temperatures. The pole figure for (573-68-293) was unique in that it represented a "single crystal" texture. The crystalline regions at these moulding conditions are very highly oriented with the *a*- and *b*-axis lying at 45° to the injection moulded bar surface.

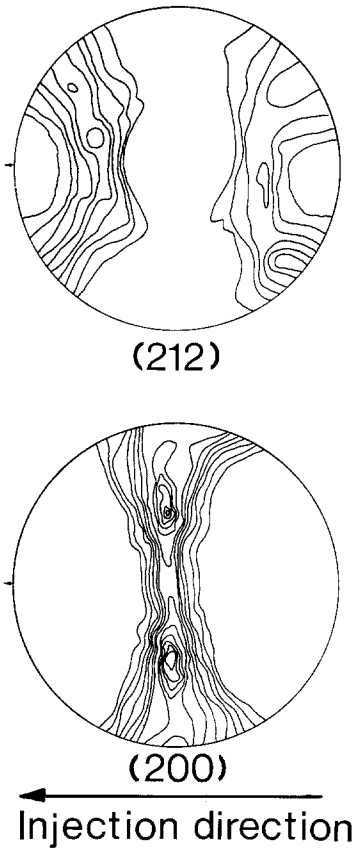

Figure 17 The (200) and (212) pole figures for region I of the material moulded at 573-68-293.

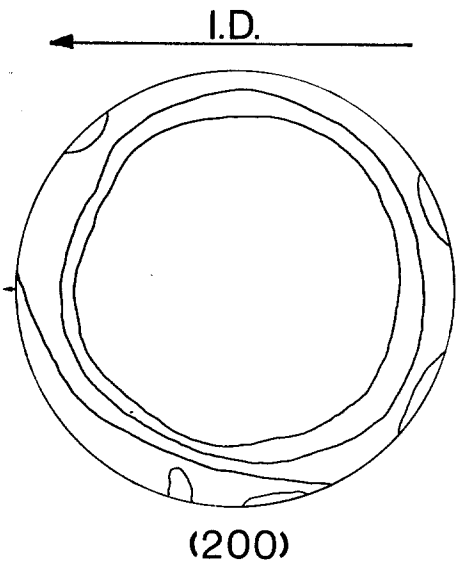

Figure 18 The (200) pole figure for region V of the material moulded at 613-68-293.

The (200) pole figures shown in Figs. 15 and 16 indicate that the molecular chain axis was parallel to the injection direction; this was confirmed unambiguously from (212) pole figures. Fig. 17, for example, shows the (212) pole figure for region I of the material moulded at (573-68-293) with the poles approximately 39° from the injection direction, supporting the parallelism of the injection direction and the *c*-axis preferred direction.

The bars moulded at (613-68-293) exhibited differences in texture and morphology not located for any other moulding. A uniquely oriented structure present in these moulded bars is that which has been annotated as region V and a high magnification scanning electron micrograph of this region is shown in Fig. 13d. The corresponding (200) pole figure presented in Fig. 18 marks the molecular chain axis for structure V as being predominantly normal to the injection direction. The *a*- and *b*-axes were contained predominantly in the plane normal to the molecular chain axis but showed no preferred orientation within that plane. The preferred orientation of the molecular chain axis in region V accounts for the unexpected microhardness and high resolution microscopy results which were obtained in these (613-68-293) bars and described in Sections 4.2 and 4.3 respectively.

4.5. Bend tests

For all of the 18 moulding conditions set out in Fig. 3, specimens were prepared for three point bend testing, and subsequently tested under the conditions set out in Section 3.3. Fig. 19 shows the resulting stress whitening and crazing for the specimens (533, 553, 573, 593, 613)-68-293. It was found that:

(a) the volume of the stress whitening region observed decreases as the barrel temperature was raised, reached its nadir at 573 K, then increased again;

(b) profuse crazing occurred in the specimens moulded at 613 K, and was responsible for the brittle failure of the specimens tested to higher strains. Fig. 20 shows the crazing of specimen 613-68-293 in greater detail;

(c) the deformation in all specimens tended to be banded, with whitening always occurring between 1 and 1.2 mm from the top surface and between 0.8 and 0.6 mm from the same surface. Additional bands at characteristic positions

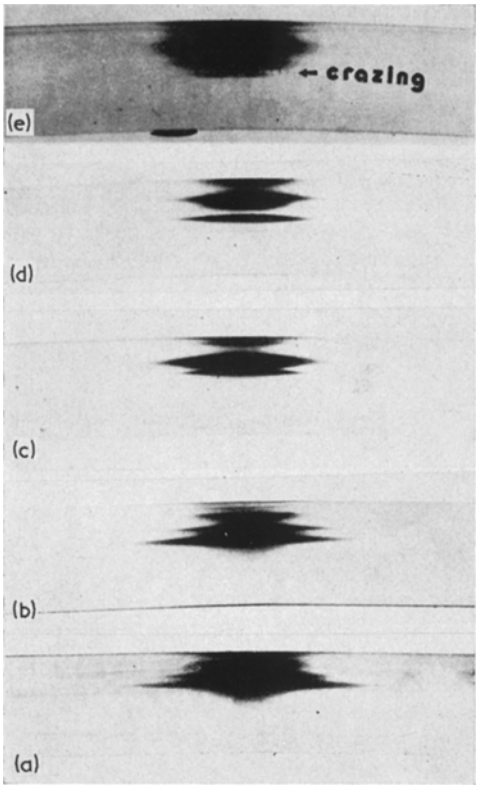

Figure 19 Using transmitted light, the stress whitening and crazing produced by bend testing the as-moulded bars for moulding at (533, 553, 573, 593 and 613)-68-293, (a) to (e) respectively. The thickness of the bars is about 3.15 mm.

occurred under certain moulding conditions.

The material moulded at (613-68-293) crazed and failed in a brittle manner. The position at which the crazes nucleated was measured and was found to be within that region of the specimen where the molecular chain axis was normal to the injection direction (region V). The molecular orientation relative to the applied strain geometry in the bend test was similar to that described previously [7] where TPX failed through a crazed controlled brittle fracture process. The presence of the material oriented perpendicular to the injection direction can arise, as noted, from changing the moulding conditions, and this structure can lead to premature brittle failure of a component.

5. Concluding remarks

The experimental results presented have demonstrated that microhardness measurements, selective etching and X-ray pole figures can all be used effectively for the characterization of microstructural changes throughout injection moulded components of semicrystalline thermoplastics. Excellent correlation exists between all three techniques for identifying changes in microstructure. X-ray pole figures can provide the most detailed information about crystalline texture; etching provides a wide canvas of the changes in microstructure throughout a component without the need for sophisticated analytical equipment; microhardness plots detail changes in microstructure speedily and with the minimum of specimen preparation.

The use of the techniques described above have shown that regions of widely differing texture occur within an injection moulded component. The variations in the positions and the extents of these regions was shown to be a

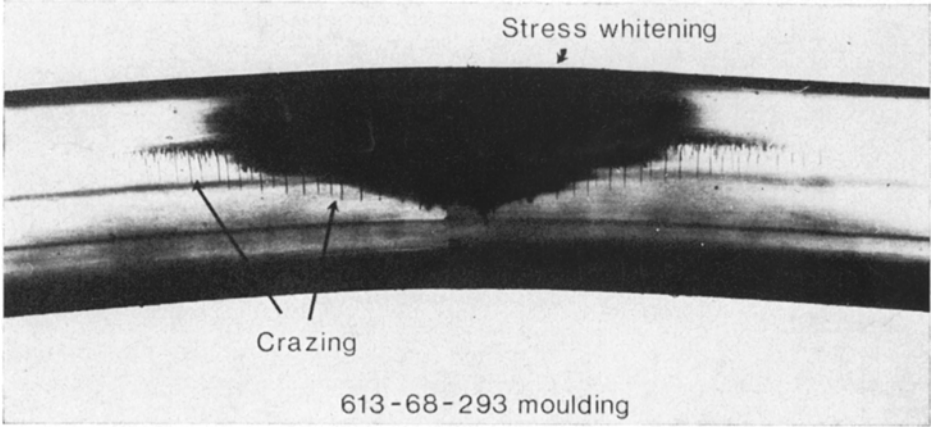

Figure 20 Using transmitted light, an enlarged view of the crazing and stress whitening for bend testing the bar moulded at 613-68-293. The position of the crazing is in that of region V.

strong function of barrel temperature, compared with mould temperature and the investigated injection pressure, both of which had little effect. The distribution of the regions exhibiting different microstructures varied in a systematic way with moulding conditions. It is to be noted, however, that the majority of moulding conditions produced a multilayer structure (see Fig. 4), a type of structuring which has been observed in amorphous polymers [20, 21] although Wales *et al.* suggested the layering could be an artifact. Clearly, this multilayer structure must be related to the mould filling process and will be developed by the variation in the shear rates through the thickness of the cavity, and by the amount of heat the polymer possesses on entry into the cavity thickness.

The distribution of structures with respect to moulding conditions indicates that it is possible to produce a preferred molecular orientation which accommodates the internal stresses imposed by the shrinkage of the component on cooling. This texture has been shown to be responsible for the marked deterioration in mechanical performance with injection moulding conditions and, therefore, demonstrates that it is possible to correlate processing conditions, microstructure and mechanical performance in injection mouldings of TPX.

The experimental procedures described can be applied to most semi-crystalline polymers and are potentially valuable methods for the design and quality control of components fabricated from semicrystalline polymers.

Acknowledgements

The authors wish to acknowledge the support given by the Science Research Council, the University of Liverpool and TBA Industrial Products Ltd, the latter being for use of injection moulding facilities. The authors are indebted to Professor D. Hull and Dr T. Owen for valuable discussions.

References

1. F. C. FRANK, A. KELLER and A. O'CONNOR, *Phil. Mag.* **4** (1959) 200.
2. E. S. CLARK, *Plastic Engineers J.* **23** (1969) 46.
3. M. R. KANTZ, H. D. NEWMAN JUN and F. H. STIGALE, *J. Appl. Polymer Sci.* **16** (1972) 1249.
4. B. HEISE, H. G. KILIAR, G. LÜPKE, P. SCHULZ, W. WOEBEKER and J. ZÖHREN, *Kolloid Z. u. Z. Polymere* **250** (1972) 120.
5. D. R. FITCHMUN and Z. MENCIK, *J. Polymer Sci.* **11** (1973) 951.
6. Z. MENCIK and D. R. FITCHMUN, *ibid* **11** (1973) 973.
7. T. W. OWEN and D. HULL, *Plastics and Polymers* **42** (1974) 19.
8. See G. DIETER JUN, "Mechanical Metallurgy" (McGraw-Hill, 1961).
9. A. J. PERRY and D. J. ROWCLIFFE, *J. Mater. Sci.* **8** (1973) 904.
10. M. A. ROTHWELL, *J. Appl. Crystallog.* **4** (1971) 494.
11. J. E. PREEDY and E. J. WHEELER, *Nature Physical Science* **236** (1972) 60.
12. D. LEWIS, E. J. WHEELER, W. F. MADDONS and J. E. PREEDY, *J. Appl. Crystallog.* **4** (1971) 55.
13. B. D. CULLITY, "Elements of X-ray Diffraction" (Addison Wesley, 1956).
14. L. E. ALEXANDER, "X-ray Diffraction Methods in Polymer Science" (John Wiley, 1969).
15. A. W. CHRISTIANSEN, J. LILLEY and J. B. SHORTALL, *Fibre Sci. and Tech.* **7** (1974) 1.
16. M. R. MACKLEY and A. KELLER, *Polymer* **14** (1973) 16.
17. J. DLUGOSZ, D. T. GRUBB, A. KELLER and M. B. RHODES, *J. Mater. Sci.* **7** (1972) 142.
18. F. A. SEYER and B. HLARÁČEK, *Kolloid Z. u. Z. Polymere* **251** (1973) 108.
19. E. S. CLARK and C. A. GARBER, *Int. J. Polym. Mat.* **1** (1971) 31.
20. J. L. S. WALES, I. R. J. VAN LEEUWER and R. VAN DER VIJGH, *Polymer Eng. and Sci.* **12** (1972) 358.
21. L. CAMWELL and D. HULL, unpublished work.

Received 24 June and accepted 5 July 1974.